https://dx.doi.org/10.1016/j.scitotenv.2021.148638

Primary emissions and secondary production of organic aerosols from heated animal fats

Liyuan Zhou[1], Tengyu Liu[2*], Dawen Yao[3], Hai Guo[3], Chunlei Cheng[4] and Chak K. Chan[1*]

[1]School of Energy and Environment, City University of Hong Kong, Hong Kong, China

[2]Joint International Research Laboratory of Atmospheric and Earth System Sciences, School of Atmospheric Sciences, Nanjing University, Nanjing, China

[3]Department of Civil and Environmental Engineering, The Hong Kong Polytechnic University, Hong Kong, China

[4]Institute of Mass Spectrometry and Atmospheric Environment, Guangdong Provincial Engineering Research Center for on-Line Source Apportionment System of Air Pollution, Jinan University, Guangzhou, China

Correspondence to: Chak K. Chan (Chak.K.Chan@cityu.edu.hk) and Tengyu Liu (tengyu.liu@nju.edu.cn)

Keywords

Cooking emissions, oxidized organic aerosol formation, urban pollution, atmospheric oxidation, aerosol mass spectrometry

Synopsis

Photooxidation of emissions from heated animal fats may be an important potential source of urban secondary organic aerosols.

Abstract

Cooking is an important source of primary organic aerosol (POA) in urban areas, and it may also generate abundant nonmethane organic gases (NMOG), which form oxidized organic aerosol (OOA) after atmospheric oxidation. Edible fats play an important role in a balanced diet and are part of various types of cooking. We conducted laboratory studies to examine the primary emissions of POA and NMOG and OOA formation using an oxidation flow reactor (OFR) for three animal fats (i.e., lard, beef and chicken fats) heated at two different temperatures (160 and 180 °C). Positive matrix factorization (PMF) revealed that OOA formed together with POA loss after photochemical aging, suggesting the conversion of some POA to OOA. The maximum OOA production rates (PRs) from heated animal fats, occurring under OH exposures (OHexp) of 8.3-15 $\times 10^{10}$ molecules cm^{-3} s, ranged from 8.9 to 24.7 μg min^{-1}, 1.6-14.5 times as high as initial POA emission rates (ERs). NMOG emissions from heated animal fats were dominated by aldehydes, which contributed 14-71% of the observed OOA. We estimated that cooking-related OOA could contribute to as high as ~10% of total OA in an urban area in Hong Kong, where cooking-related organic aerosols (COA) dominated the POA. This study provides insights into the potential contribution of cooking to urban OOA, which might be especially pronounced when cooking contributions dominate the primary emissions.

1 Introduction

Organic aerosol (OA) contributes 20-90% of the submicron particulate mass in the atmosphere[1, 2], which influences air quality, climate and human health[3]. OA is a complex mixture comprising both primary organic aerosol (POA) emitted directly from sources and secondary organic aerosol (SOA) formed via atmospheric oxidation of volatile organic compounds (VOC). Currently, the sources of

POA are relatively well identified, while the formation and characteristics of SOA remain as an open and active research field. Cooking-related organic aerosols (COA), commonly recognized as primary species, have been found to represent 10 - 35% of the total OA measured in urban locations[4-10]. Cooking contributions in organic aerosol even exceeded those from vehicles in urban Hong Kong[4, 5]. In addition to OA emissions, numerous gaseous pollutants are also produced from cooking. Klein et al. [11] investigated the nonmethane organic gases (NMOG) emissions from a broad variety of cooking styles and techniques and found that methanol dominated the emissions from boiling vegetables and aldehydes dominated the emissions from the frying and charbroiling processes. Large amounts of aldehydes were also found during heating culinary oils and fats[12-15] and they dominated VOC emissions from lard fat- or olive oil-fried loin chops[16]. These aldehydes may result in detrimental health impacts, such as genotoxicity and tumorigenicity[17, 18], and potentially serve as precursors for SOA formation[19, 20].

Recent smog chamber and oxidation flow reactor (OFR) studies have demonstrated that cooking emissions can generate a large amount of SOA through photochemical aging[20-24]. Cooking SOA production has been identified from both western-style cooking, such as meat charbroiling[21], and oriental domestic style cooking[24, 25]. Liu et al. [22] observed SOA formation from gas-phase emissions of heated vegetable oils, and its formation rate could be even one order of magnitude higher than the POA emission rate[15]. Compared with vegetable oils, animal fats are known to have a higher saturated fatty acid profile. Although initial epidemiological studies have associated saturated fat intake with heart disease risk, subsequent studies have failed to confirm the link[26]. Owing to their low cost and wide availability, animal fats are widely used by food manufacturers as a food ingredient in many countries [27]. Woodgate et al. [28] reported that 172 million tonnes of vegetable and animal oils and fats were produced worldwide in 2013, from which a non-negligible

amount of 25 million tonnes (14%) were of animal origin. In particular, animal fats are widely used for frying fish and chips in Belgium and the UK[28] and as a major raw material for Chongqing hotpot in China[29]. They are also naturally related to meat cooking and are popular in the bakery industry for bread and pastry making[28]. SOA formation from emissions of heated vegetable oils has received growing attention from researchers[15, 20, 22, 23, 30]; however, the magnitude and composition of SOA formed from emissions of heated animal fats are rarely studied.

In this study, we characterized both fresh and aged OA emissions from heated animal fats and compared those to the emissions from heated vegetable oils. NMOG emissions and their potentials to form oxidized OA (OOA) are evaluated and discussed. Here, OOA includes both oxidized POA and SOA formed from gaseous precursors.

2 Materials and methods

2.1 OFR experiments

Photooxidation experiments were performed on emissions from three heated animal fats in an OFR Gothenburg Potential Aerosol Mass Reactor, Go: PAM, which has been described in detail elsewhere[31, 32]. Briefly, Go: PAM is a 7.2 L cylindrical continuous-flow quartz glass flow reactor, equipped with one Philips TUV 30 W fluorescent lamp (λ=254 nm). Hydroxyl radicals (OH) were generated through O_3 photolysis irradiated by the UV lamp in the presence of water vapor to simulate photochemical oxidation in the atmosphere. O_3 was produced by an O_3 generator (Model 610, Jelight Inc. USA) with pure oxygen supplied. A schematic of the experimental setup was shown in Figure S1 (Supporting Information, SI). The tested animal fats include lard, beef and chicken fats. For each experiment, animal fat was melted, and a sample of 250 mL was heated at approximately 180 or 160 °C, associated respectively with standard and lower-bound temperatures

of frying practices[13, 33, 34], in a 500 mL glass bottle in a dimethyl silicone oil bath. The emissions were firstly diluted by zero air by a factor of approximately 46, then ~ 0.3 L min^{-1} of the diluted flow was introduced to the Go: PAM chamber with a final dilution factor of several hundred to one thousand. The total flow in Go: PAM was around 6.3 L min^{-1}, resulting in a residence time of ~ 70 s. The relative humidity (RH) and temperature in the reactor were measured continuously and stabilized at 77-80 % and 17-19 °C, respectively. The control of RH was achieved by passing pure N_2 and O_2 through water bubblers. The OH levels were controlled by varying the input O_3 concentrations, which were adjusted to four different levels, ranging from 0.52 to 6.6 ppm. Fresh emissions were measured in the absence of O_3 and with UV lamp off, and aged emissions were subsequently characterized when OH radicals were produced.

Size-dependent particle wall losses in Go: PAM have been quantified by Watne et al. [32], the transmission efficiency for particles with mobility diameters (d_m) larger than 25 nm was higher than 90%. The particles larger than 25 nm accounted for greater than 97% of the aerosol mass in both fresh and aged animal fat emissions, and the wall loss of particles was calculated to be generally less than 2%. No correction for this was made.

2.2 Characterization of Gas- and Particle-phase chemical compositions

NMOGs were characterized using an online proton transfer reaction - mass spectrometry (PTR-MS, PTR-QMS500, IONICON Analytik GmbH, Innsbruck, Austria)[35]. The observed NMOG masses were assigned to the most likely compounds based on knowledge of the typical NMOG emissions from cooking oils[11, 15], with a caveat that other compounds might be superimposed on the same nominal mass. The calibration and operation of this instrument have been discussed elsewhere[36]. Even though PTR-MS relies on soft ionization of chemical species by protonation

with H_3O^+, some degrees of fragmentation may still occur for many compounds present in cooking emissions (e.g., aldehydes)[37]. Fragmentation patterns of aldehydes were estimated from literature[11, 15] and the corresponding corrections were applied to NMOG emissions in this study (Table S1). The OH concentrations inside the OFR were determined from the decay of acrolein[15, 38]. The estimated OH exposures (OHexp) ranged from 6.7×10^9 to 1.5×10^{11} molecules cm^{-3} s, equivalent to 1.2 h to 1.2 days of photochemical aging, assuming a 24 h average ambient OH concentration of 1.5×10^6 molecules cm^{-3} [39]. Acrolein was measured to constitute around 88-96% of the unit mass signal at m/z 57 $[M+H]^+$ in the NMOG emissions from heated canola and sunflower oils (180-200°C) as measured with a time-of-flight PTR-MS[11]. Therefore, by assuming similar contributions of acrolein with potential interferences of butylene, the OHexp in this study maybe 3-8% overestimated.

Particle number concentrations and size distributions were measured by a customized scanning mobility particle sizer (SMPS), which is the combination of a differential mobility analyzer column (DMA, model 3081, TSI Inc. USA) with flow controls and a condensation particle counter (CPC, model MAGIC200, Aerosol Dynamics Inc. USA). When calculating particle mass, particle sphericity and an aerosol density of 1.4 g cm^{-3} [40] were assumed. The chemical composition of submicron non-refractory particulate matter (NR-PM_1) was characterized by a high-resolution time-of-flight aerosol mass spectrometer (hereafter AMS, Aerodyne Research Inc. USA)[41]. The instrument was operated in high-sensitivity V mode and high-resolution W mode alternating every 2 min. Since the OA from heated animal fats is likely liquid, the collection efficiency (CE) of 1 was applied in this study. This would to some extent compensate for the potential overestimation of OA concentrations attributed to the higher relative ionization efficiency (RIE) for COA of 1.56-3.06 than the default value of 1.4[42]. The particle mass concentrations

measured by AMS and SMPS showed a good correlation (relative difference around 9%, R^2= 0.97) (Figure S2). The toolkit Squirrel 1.62F and Pika 1.22F were used in Igor (Wavemetrics Inc. USA) to analyze the AMS data. The molar ratios of hydrogen to carbon (H:C) and oxygen to carbon (O:C) were determined with the improved-ambient method[43]. For better comparison, the ambient related elemental ratio with original Aiken calibrations[44, 45] in previous studies were multiplied by a ratio of 1.27 to the O:C and 1.11 to the H:C according to Canagaratna et al. [43] in this study, resulting in 27% and 11% higher than their originally reported values.

2.3 POA emission rate and OOA production rate

Emission rates (ER) and production rates (PR) were commonly used for the description of the amount of primarily emitted and secondarily produced compounds from cooking activities[22, 46-48]. Here, micrograms (μg) of NMOG or POA emitted, or OOA produced per minute (min) from heated animal fats were calculated using the following equation:

$$ER_{NMOG\ or\ POA}\ or\ PR_{OOA} = [NMOG\ or\ OA] \times DR \times F, \quad (1)$$

where [NMOG or OA] is the concentration of NMOG or OA in μg m^{-3}, DR is the dilution ratio and F is the flow rate of carrier gas in $m^3\ min^{-1}$. The adoption of ER or PR compensates for different degrees of dilution during measurements, enabling a direct comparison with the previously reported cooking emission data.

3 Results and Discussion

3.1 Primary emissions

Figure 1 shows the NMOG and POA emissions from heated animal fats (lard, beef and chicken fats) at 160 and 180°C. The NMOGs were classified into eight families: alkanals, alkenals,

alkadienals, carboxylic acids, alcohols, O- containing, N- containing, and others. Alkadienals were not directly measured in this study. Heptadienal has been reported as the most dominant alkadienals[15, 20] and its concentration was estimated according to its good correlation with acrolein (R^2=0.97) from emissions of heated vegetable oils[15] (Figure S3). The "O-containing" family are compounds not attributable to the other families but contain oxygen. A similar definition applies to the "N-containing" family. The "Others" family denotes hydrocarbon fragments (see details in Table S2). Note that the ERs of NMOGs were presented on a logarithmic scale to reflect the contributions of the lowly emitted families. Heated lard had the highest NMOG emissions at both temperatures, followed by beef fat, and lastly the chicken fat. The NMOG ERs for lard were 2.4 - 3.3 times that of chicken fat at the respective temperatures. When the heating temperature increased from 160 to 180°C, ERs of NMOG were enhanced by 3.4 - 6.8 times for the three fats. In general, the heating temperature played a more critical role than fat types in affecting NMOG ERs in this study. Liu et al. [15] reported variability in the ERs of NMOG ranging from 281 to 2612 μg min^{-1} for various heated vegetable oils (sunflower, olive, peanut, canola, soybean and palm oils) at 200°C. Slightly lower temperatures (160 or 180°C) were used for heating animal fats because their smoke points (e.g., 190°C for lard[49]) are lower than those of vegetable oils (generally > 200°C[49]). In comparison, heated animal fats at 180°C gave similar ERs of NMOGs (539 -1321 μg min^{-1}), within the wide range of reported values from vegetable oils. Consistent with heated vegetable oils[15], charbroiling or shallow frying of meat and deep frying of fish and potato processes[11], NMOG emissions from heated animal fats were also dominated by aldehydes but with different relative compositions depending on heating temperatures and fat types. Generally, alkanals (40 - 93%), alkenals (4 - 28%) and alkadienals (1 - 11%) together accounted for more than 93% of NMOG emissions for most of the experiments, except for heated chicken fat at 160°C,

where they only contributed 79%. Large amounts of aldehydes were likely formed from the oxidation of unsaturated fatty acids during heat treatments, while saturated fatty acids were more resistant to oxidation[50]. Animal fats generally have lower contents of unsaturated fatty acids (around 60%) than vegetable oils (80-90%), except for coconut and palm oils (9-50%)[51]. Hence, they are expected to produce less aldehydes. However, Chyau et al. [52] reported the highest amounts of hexanal, nonanal, heptenal, and even total VOCs in deep-fried shallot flavorings prepared with lard, instead of soybean and corn oils in pot cooking at 150-160°C. Similarly, heated lard had a higher emission of the total polar lipophilic aldehydes than peanut and canola oils[53]. It was postulated that some compounds in animal fats might catalyze the peroxidation process to form aldehydes[53].

Figure 2 shows the speciation and distribution of aldehydes from heated animal fats. High abundances of butanal, pentanal, hexanal, and heptanal were observed in alkanal emissions (open circles), and acrolein dominated the alkenal emissions (closed triangles). Large amounts of these compounds with different relative abundances have also been observed previously in the cooking fumes of various animal fats and vegetable oils[11, 12, 15, 18, 50, 54, 55]. The different relative abundances of aldehydes may be associated with the composition of fatty acids in cooking oils. For example, linoleic acid is commonly assumed to associate with the formation of pentanal and hexanal[56-58], while Chen et al. [59] found abundant emissions of these aldehydes from fried oleic acid. The contents of linoleic and oleic acid vary, but their sum was similar for the three animal fats (50-57%)[51]. Also, acrolein may be formed through the degradation of glycerol[60]. Temperatures may also play a role in different aldehyde profiles as the dependence with temperature was more evident for alkanal than alkenal emissions[56].

Consistent with NMOG emissions, the emissions of POA were increased at higher heating temperatures (Figure 1). Heated beef fats yielded the largest amount of POA, and followed by chicken fats, while lard had the lowest POA ERs with almost zero emissions at 160°C. The average particle number size distributions of lard emissions were bimodal, with a dominant mode peaking at ~30nm and the other mode peaking at ~100 to 200 nm, whereas those of beef and chicken fats were dominated by the latter mode (Figure S4).

3.2 POA-OOA split

Figure 3a shows measured OA from heated beef, lard and chicken fats at 160 and 180 °C as a function of OHexp. OA ER was enhanced after photochemical aging. It reached a maximum as early as 0.35×10^{11} molecules cm^{-3} s (around 6.5 h) for 180 °C beef fat but was still on the rise even after 0.8-1.2 days equivalent of aging for lard at both temperatures. Compared with the initial ERs, the maximum OA ERs increased by 1.8 times or more after several hours to 1.2 days of aging. Animal fats heated at 180 °C exhibited faster and larger OA increases than those at 160 °C, as reflected by a steeper slope in the OA evolution. This is likely due to the higher abundance of SOA precursors at a higher heating temperature (Figure 1).

To further explore the sources and formation processes of OA, we performed positive matrix factorization (PMF) analysis on each animal fat (at each temperature) OA dataset by combining data at different OHexp for statistical significance (see details in SI Figures S5-10). Generally, two factors were identified for most of the datasets, including one POA factor and one oxygenated organic aerosol (OOA) factor. The only exception is lard at 160 °C; it has no POA factor but two OOA factors with different levels of oxidation were identified. The ratios of the total residual concentration to total OA concentration were less than 3% (Figures S5-10). PMF solutions with

more factors yield a mixed factor with both POA and OOA components (Figure S11), thus does not improve the PMF performance. For all animal fats, the most prominent peaks in mass spectra (MS) of PMF-derived POA factors were observed at m/z 41, 43 and 55 (Figure S12). The most abundant fragments in these unit masses were dominated by $C_3H_5^+$, $C_3H_7^+$ and $C_4H_7^+$ ions. In contrast, PMF-derived OOA factors have dominating peaks of m/z 28, 29, 43 and 44, corresponding to CO^+, CHO^+, $C_2H_3O^+$ and CO_2^+, respectively. The θ angles between the MS of POA factors of different animal fats were 4-14° (Figure S13). Generally, a θ of 0-5, 6-10, 11-15, 16-30, and > 30° (corresponding to an R^2 ranging approximately 1 to 0.99, 0.98 to 0.97, 0.96 to 0.93, 0.92 to 0.75 and <0.75 respectively) indicates an excellent match, good match, many similarities, limited similarity and poor match, respectively, between the two spectra[21, 61]. The MS of OOA factors of different animal fats exhibited excellent to limited similarities (θ =5-23°), which may be due to different degrees of photochemical aging. Generally, the significant increase of oxygen-containing ions in OOA factors indicated the formation of the more oxidized organic aerosols. The separation of factors was reasonable with an excellent agreement (θ< 5°) between directly measured POA MS and PMF-derived POA factor spectra (Figure S13).

The average POA spectrum of animal fats was compared with that of laboratory-generated cooking OA[23, 62] and PMF COA factors from ambient measurements[5-7, 63-69] from previous studies (Figure 4a). The MS of average animal fat POA exhibited many similarities (θ =13°) with that of palm oil POA[23], and it has good agreement with different ambient COA factors derived from urban areas in Hong Kong[5], Beijing[66], Rome[65] and Oakland[63] with θ ranging from 14 to 19° (Figure 4a). This is probably due to the heating of fats in western and Asian style cooking of meat. On the other hand, while ambient COA factors in Barcelona urban background[7] and Pasadena urban area[68] had limited correlations with animal fat POA MS, they displayed relatively better agreements with the

255 average animal fat PMF OOA factor (Figure 4a). This highlights the influence of atmospheric
256 oxidation conditions on ambient COA factors. Angles between the average animal fat PMF OOA
257 factor and ambient PMF OOA factors[5, 7, 64-66, 68-71] were in the range of 11 - 46° (Figure 4b). The
258 highest similarity of 11° was observed with the OOA factor reported by Lee et al. [5] from the urban
259 Mong Kok site in Hong Kong, where COA contributed to 34.6% of OA, even more than that of
260 traffic POA (26.4%).

261 Figures 3b and 3c show the evolution of PMF resolved POA and OOA factors with OHexp.
262 The ERs of animal fat POA factors decreased by 68% to more than 90% after 0.6 -1.2 days of
263 photochemical aging, which may be due to the heterogeneous oxidation of POA. Liu et al. [15]
264 reported that POA from olive oil undergoes heterogeneous reaction more readily than palm oil
265 POA. They attributed this to more abundant unsaturated organic species in olive oil, which can
266 react with OH radicals or O_3 more quickly than saturated species[72]. The unsaturated fatty acid
267 contents of animal fats used in this study generally fell in between that of olive and palm oils[51].
268 The OH oxidation of unsaturated hydrocarbons occurs either by the abstraction of an H atom or
269 by the addition of OH to the C=C double bond, while that of saturated hydrocarbons is initiated
270 solely by the H abstraction[73]. In addition, Molina et al. [74] reported the full volatilization of a
271 monolayer of C_{18} organic species following the heterogeneous loss of only 2 to 3 OH collisions.
272 Kaltsonoudis et al. [21] also observed an evident decay of meat charbroiling POA due to
273 heterogeneous reaction.

274 The amounts of OOA formed from the oxidation of emissions from heated animal fats
275 increased substantially with photochemical aging (Figure 3c). The maximum OOA PRs ranged
276 from 8.9 to 24.7 μg min^{-1} and, specifically, 14.5 times as high as initial POA ER for 180 °C lard,
277 followed by chicken and beef fats with enhancements of 1.6 - 3.4. These OOA to POA ratios

generally fell within previously reported ranges for vegetable oils heated at 200 °C, from 0.7 for olive oil to 60 for sunflower oil[15] (Figure S14). It should be noted that, in Liu et al. [15]'s study, the precursors from vegetable oils were oxidized in the smog chamber at photochemical age of 1.9 h, lower than that in this study. However, due to longer residence time to allow complete condensation of semi-volatile species into SOA, chamber studies have been found to give a higher SOA yield than flow reactor of equivalent OHexp[75]. In this study, functionalization reactions may play a leading role in the formation of OOA, as reflected by the continuous increase of OOA PRs. However, fragmentation may be important in the growth of beef fat OOA at 180°C. Overall, compared with the initial POA ERs, the OOA formation potential, represented as the maximum OOA PR, varied less for different animal fats at the same temperature (Figure S14).

3.3 Contributions of individual NMOGs to observed OOA

The OOA production from oxidation of each speciated precursor in the NMOG mix was estimated by multiplying the reacted precursor i at a certain OHexp and the corresponding mass yields Y_i reported in the literature[20, 72, 76-79]:

$$OOA_{estimated} = \sum_i [NMOG]_i \times (1 - \exp(-k_i[OH]t)) \times Y_i \quad , \qquad (2)$$

where $[NMOG]_i$ is the mass concentration of precursor i before photooxidation, and k_i is its corresponding OH reaction rate constant. The values used for k_i and Y_i were presented in Table S3. Liu et al. [15] identified alkenals as the major precursors to the observed vegetable oil SOA in PTR measurements. Although the SOA mass yields for < C_{11} alkanals were generally less than 0.02 for a maximum C_{OA} ~ 10 μg m^{-3} [80], the latest study by Takhar et al. [20] revealed that heptanal contributed 7% to the observed canola oil SOA (only C_7 to C_{10} aldehydes were quantified in their Tenax tube study). Hence, due to the significant abundances in NMOG emissions, pentanal, hexanal and

heptanal were also included in our analysis. Chacon-Madrid et al. [80] reported no significant difference between SOA mass yields for C_5, C_8 and C_{11} alkanals, and therefore we assumed the SOA yields of all alkanals are the same as that of heptanal in Takhar et al. [20]. Available data of SOA yields from various aldehydes precursors is still scarce, and hence future studies are warranted. Figure 5 shows the estimated contributions of individual alkenals and the three most abundant alkanals to the observed OOA. Alkenals accounted for 4-21% of the observed OOA, comparable to fractions of 8-55% in vegetable oil experiments reported by Liu et al. [15]. Incorporating the alkanals increased the explained contributions of OOA, 14% for chicken fat at 160 °C to 71% for lard fat at 180 °C. Over the experiments, the contributions of individual aldehydes to observed OOA were highly variable. Acrolein and hexanal, the most prominent compounds present in alkenal and alkanal emissions, contributed to 6 % and 39 % of the observed OOA for lard fat at 180 °C but only 1 % and 19 % for beef fat at 180 °C. In general, these aldehydes accounted for larger OOA fractions when animal fats heated at higher temperatures, likely related to their higher abundances. The unexplained OOA may be attributed to the oxidation of POA itself or fragments from heterogeneous reactions of the POA. Unidentified semi-volatile and intermediate-volatility organic compounds (SVOCs and IVOCs) from cooking emissions may also play a role in forming OOA[15].

3.4 Chemical evolution of OA

In Figure 6, H:C and O:C ratios of OA from heated animal fats were compared to those reported from laboratory cooking emission studies of vegetable oils[23], meat frying[24] or charbroiling[21] and Asian cuisine[24] and ambient PMF COA and OOA factors[4, 5, 21, 65, 66, 69, 81, 82] in a Van Krevelen diagram. The H:C and O:C were 1.88-2.03 and 0.14-0.19 for animal fat POA, consistent with those

of cooking POA reported in previous laboratory studies[21, 23, 24] (H:C: 1.80-2.10, O:C: 0.09-0.21) (black markers, color scaled by OHexp) and ambient COA factors[4, 5, 21, 65, 66, 69, 82] (grey markers) (H:C: 1.75-1.96, O:C: 0.10-0.27). The H:C versus O:C trend of our animal fat OA dataset fell on a line with a slope of -0.24 (dark blue dashed line), which is comparable to that of -0.19 for heated canola oil SOA in Takhar et al. [20]. This implies the formation of both alcohol or peroxide and carboxylic acid in animal fat OOA. However, this slope is far from those of the ambient OA dataset (slope ≈ -0.7 to -1) (pink and dark red markers)[5, 7, 21, 65, 66, 69, 81]. Interestingly, for the ambient measurements in urban Mong Kok, Hong Kong[5], where cooking contributions in POA exceeded those related to vehicles, the evolution of the COA factor to one of the three resolved OOA factors (varying oxygenation) was linear with a slope of -0.19 (light blue dashed line). This agrees well with the animal fat OOA evolution in our study, which might suggest this specific OOA factor is likely dominated by the aged cooking-related OA. This is also supported by its highest MS similarity among all the ambient OOA factors with the average animal fat PMF OOA factor (θ =11°) (details in Sect. 3.2 and Figure 4b). On the other hand, COA generally accounted for a small fraction of OA in suburban areas. For example, COA contributed to less than 10% of total OA in HKUST Supersite[82], and the OA evolution followed a line with a slope of around -1. A recent study near the entrance of a tunnel in Hong Kong yielded a slope of -0.64 from the COA factor to the OOA factors[4].

3.5 Atmospheric implications

Cooking and traffic emissions were dominant pollution sources in urban areas[5-7, 83], among which traffic emissions have been continually decreasing over the years[4] with the implementation of increasingly stringent regulations, such as the adoption of cleaner engines and cleaner fuels[32, 84-

[86]. However, cooking emissions are barely regulated, and the contribution of cooking to urban SOA is still poorly understood. Cooking involving the heating of vegetable and animal oils and fats is common in preparing foods in numerous cultures[87]. Our earlier works[15, 22, 23] have studied the emission characteristics from heated vegetable oils and demonstrated that SOA formed from oil emissions likely exceeded corresponding POA emissions. Here, we investigated primary emissions and secondary production of gas- and particle-phase pollutants from heated animal fats, and evaluated their similarities and differences with those of vegetable oils. Heated animal fats at 180°C gave a similarly wide range of ERs of NMOGs (539 -1321 μg min^{-1}) to those of vegetable oils at 200°C. Cooking at a lower temperature (160°C) could be efficient in eliminating NMOGs emissions (3.4 - 6.8 times lower than those at 180°C). As the most dominant class of NMOGs emitted from heated animal fats, aldehydes may play an important role in forming cooking SOA. We observed that atmospheric oxidation of animal fat OA involved the formation of OOA accompanying POA loss, with net OA reaching its maximum value (1.8 times or more than the initial POA) after several hours to 1.2 days equivalent of aging.

We further revealed that potential OOA from cooking emissions might play an important role in urban areas where cooking contributions dominate the primary emissions. Cooking exceeded traffic as the major source of POA in Lee et al. [5]'s measurements in urban Mong Kok, Hong Kong. One of three resolved OOA factors from their study has relatively high similarities with animal fat OOA in this study regarding the mass spectrum (θ =11°) and oxidation mechanisms (slope of -0.19 in Van Krevelen diagram). This specific OOA factor might therefore be dominated by cooking emissions. Based on this assumption, we estimate that cooking might contribute as high as 44.1 % of total OA at the urban Mong Kok site. Therein, primary COA and cooking-related OOA contributed 34.6% and 9.5%, respectively. Future studies are encouraged to employ the mass

spectra of OOA formed from heated animal fats and other various cooking styles and techniques to constrain the OA source apportionments and further estimate the contribution of cooking OOA in ambient air.

ASSOCIATED CONTENT

Supporting Information

Schematic of the experimental setup (Figure S1), comparison between AMS mass vs. SMPS mass (Figure S2), emission rates of heptadienal and acrolein from vegetable oils (Figure S3), average particle number size distributions for fresh and aged particles (Figure S4), diagnostic plots of the PMF analysis (Figures S5-10), comparisons of two-factor and three-factor solutions of PMF analysis (Figure S11), mass spectra for PMF resolved POA factor, OOA factor and the difference between the two factors (Figure S12), θ between directly measured POA mass spectra and PMF resolved POA and OOA factor spectra (Figure S13), comparisons of POA emission rates and captured maximum OOA production rates for animal fats and vegetable oils (Figure S14), fragmentation table of the most abundant aldehydes (Table S1), assigned ions and families for all detected m/z of PTR-MS (Table S2), and OH reaction rate constants of alkenals and alkanals and applied SOA yields data (Table S3).

Notes

The authors declare no competing financial interest.

Acknowledgment

We gratefully acknowledge support from the Guangzhou Development District International Science and Technology Cooperation Project (No. 2018GH08), the University Strategic Importance scheme (1-ZE1M) and the Strategic Focus Area scheme of The Research Institute for Sustainable Urban Development (1-BBW9) at The Hong Kong Polytechnic University.

References

1. Zhang, Q.; Jimenez, J. L.; Canagaratna, M. R.; Ulbrich, I. M.; Ng, N. L.; Worsnop, D. R.; Sun, Y., Understanding atmospheric organic aerosols via factor analysis of aerosol mass spectrometry: a review. *Analytical and bioanalytical chemistry* **2011,** *401*, (10), 3045-3067.
2. Jimenez, J. L.; Canagaratna, M.; Donahue, N.; Prevot, A.; Zhang, Q.; Kroll, J. H.; DeCarlo, P. F.; Allan, J. D.; Coe, H.; Ng, N., Evolution of organic aerosols in the atmosphere. *Science* **2009,** *326*, (5959), 1525-1529.
3. Hallquist, M.; Wenger, J. C.; Baltensperger, U.; Rudich, Y.; Simpson, D.; Claeys, M.; Dommen, J.; Donahue, N.; George, C.; Goldstein, A., The formation, properties and impact of secondary organic aerosol: current and emerging issues. *Atmospheric chemistry and physics* **2009,** *9*, (14), 5155-5236.
4. Yao, D.; Lyu, X.; Lu, H.; Zeng, L.; Liu, T.; Chan, C. K.; Guo, H., Characteristics, sources and evolution processes of atmospheric organic aerosols at a roadside site in Hong Kong. *Atmospheric Environment* **2021**, 118298.
5. Lee, B. P.; Li, Y. J.; Yu, J. Z.; Louie, P. K.; Chan, C. K., Characteristics of submicron particulate matter at the urban roadside in downtown Hong Kong—Overview of 4 months of continuous high-resolution aerosol mass spectrometer measurements. *Journal of Geophysical Research: Atmospheres* **2015,** *120*, (14), 7040-7058.
6. Crippa, M.; DeCarlo, P.; Slowik, J.; Mohr, C.; Heringa, M.; Chirico, R.; Poulain, L.; Freutel, F.; Sciare, J.; Cozic, J., Wintertime aerosol chemical composition and source apportionment of the organic fraction in the metropolitan area of Paris. *Atmospheric Chemistry and Physics* **2013,** *13*, (2), 961-981.
7. Mohr, C.; DeCarlo, P.; Heringa, M.; Chirico, R.; Slowik, J.; Richter, R.; Reche, C.; Alastuey, A.; Querol, X.; Seco, R., Identification and quantification of organic aerosol from cooking and other sources in Barcelona using aerosol mass spectrometer data. *Atmospheric Chemistry and Physics* **2012,** *12*, (4), 1649-1665.

8. Ge, X.; Setyan, A.; Sun, Y.; Zhang, Q., Primary and secondary organic aerosols in Fresno, California during wintertime: Results from high resolution aerosol mass spectrometry. *Journal of Geophysical Research: Atmospheres* **2012,** *117*, (D19).
9. Sun, Y.-L.; Zhang, Q.; Schwab, J.; Demerjian, K.; Chen, W.-N.; Bae, M.-S.; Hung, H.-M.; Hogrefe, O.; Frank, B.; Rattigan, O., Characterization of the sources and processes of organic and inorganic aerosols in New York city with a high-resolution time-of-flight aerosol mass apectrometer. *Atmospheric Chemistry and Physics* **2011,** *11*, (4), 1581-1602.
10. Allan, J.; Williams, P.; Morgan, W.; Martin, C.; Flynn, M.; Lee, J.; Nemitz, E.; Phillips, G.; Gallagher, M.; Coe, H., Contributions from transport, solid fuel burning and cooking to primary organic aerosols in two UK cities. *Atmospheric Chemistry and Physics* **2010,** *10*, (2), 647-668.
11. Klein, F.; Platt, S. M.; Farren, N. J.; Detournay, A.; Bruns, E. A.; Bozzetti, C.; Daellenbach, K. R.; Kilic, D.; Kumar, N. K.; Pieber, S. M., Characterization of gas-phase organics using proton transfer reaction time-of-flight mass spectrometry: cooking emissions. *Environmental science & technology* **2016,** *50*, (3), 1243-1250.
12. Zhang, D.-C.; Liu, J.-J.; Jia, L.-Z.; Wang, P.; Han, X., Speciation of VOCs in the cooking fumes from five edible oils and their corresponding health risk assessments. *Atmospheric Environment* **2019,** *211*, 6-17.
13. Claxson, A. W.; Hawkes, G. E.; Richardson, D. P.; Naughton, D. P.; Haywood, R. M.; Chander, C. L.; Atherton, M.; Lynch, E. J.; Grootveld, M. C., Generation of lipid peroxidation products in culinary oils and fats during episodes of thermal stressing: a high field 1H NMR study. *FEBS letters* **1994,** *355*, (1), 81-90.
14. Zhang, Q.; Qin, W.; Lin, D.; Shen, Q.; Saleh, A. S., The changes in the volatile aldehydes formed during the deep-fat frying process. *Journal of food science and technology* **2015,** *52*, (12), 7683-7696.
15. Liu, T.; Wang, Z.; Huang, D. D.; Wang, X.; Chan, C. K., Significant production of secondary organic aerosol from emissions of heated cooking oils. *Environmental science & technology letters* **2018,** *5*, (1), 32-37.
16. Ramírez, M. R.; Estévez, M.; Morcuende, D.; Cava, R., Effect of the type of frying culinary fat on volatile compounds isolated in fried pork loin chops by using SPME-GC-MS. *Journal of agricultural and food chemistry* **2004,** *52*, (25), 7637-7643.
17. Chang, L. W.; Lo, W.-S.; Lin, P., Trans, trans-2, 4-decadienal, a product found in cooking oil fumes, induces cell proliferation and cytokine production due to reactive oxygen species in human bronchial epithelial cells. *Toxicological sciences* **2005,** *87*, (2), 337-343.
18. Peng, C.-Y.; Lan, C.-H.; Lin, P.-C.; Kuo, Y.-C., Effects of cooking method, cooking oil, and food type on aldehyde emissions in cooking oil fumes. *Journal of hazardous materials* **2017,** *324*, 160-167.
19. Fullana, A.; Carbonell-Barrachina, A. A.; Sidhu, S., Comparison of volatile aldehydes present in the cooking fumes of extra virgin olive, olive, and canola oils. *Journal of Agricultural and Food Chemistry* **2004,** *52*, (16), 5207-5214.
20. Takhar, M.; Li, Y.; Chan, A. W., Characterization of secondary organic aerosol from heated cooking oil emissions: evolution in composition and volatility. *Atmospheric Chemistry and Physics Discussions* **2020**, 1-24.
21. Kaltsonoudis, C.; Kostenidou, E.; Louvaris, E.; Psichoudaki, M.; Tsiligiannis, E.; Florou, K.; Liangou, A.; Pandis, S. N., Characterization of fresh and aged organic aerosol emissions from meat charbroiling. *Atmospheric Chemistry and Physics* **2017,** *17*, (11), 7143-7155.

22. Liu, T.; Li, Z.; Chan, M.; Chan, C. K., Formation of secondary organic aerosols from gas-phase emissions of heated cooking oils. *Atmospheric Chemistry and Physics* **2017,** *17*, (12), 7333-7344.
23. Liu, T.; Wang, Z.; Wang, X.; Chan, C. K., Primary and secondary organic aerosol from heated cooking oil emissions. *Atmospheric Chemistry and Physics* **2018,** *18*, (15), 11363-11374.
24. Zhang, Z.; Zhu, W.; Hu, M.; Wang, H.; Chen, Z.; Shen, R.; Yu, Y.; Tan, R.; Guo, S., Secondary Organic Aerosol from Typical Chinese Domestic Cooking Emissions. *Environmental Science & Technology Letters* **2020**.
25. Zhang, Z.; Zhu, W.; Hu, M.; Liu, K.; Wang, H.; Tang, R.; Shen, R.; Yu, Y.; Tan, R.; Song, K., Formation and Evolution of Secondary Organic Aerosol Derived from Urban Lifestyle Sources: Vehicle Exhaust and Cooking Emission. *Atmospheric Chemistry and Physics Discussions* **2021**, 1-27.
26. Cassiday, L., Big fat controversy: changing opinions about saturated fat. *Inform* **2015,** *26*, 343-349.
27. Aida, A. A.; Man, Y. C.; Wong, C.; Raha, A.; Son, R., Analysis of raw meats and fats of pigs using polymerase chain reaction for Halal authentication. *Meat science* **2005,** *69*, (1), 47-52.
28. Woodgate, S. L.; van der Veen, J. T., Fats and oils–animal based. *Food processing: principles and applications* **2014**, 481-499.
29. Tang, B.; Xi, C.; Zou, Y.; Wang, G.; Li, X.; Zhang, L.; Chen, D.; Zhang, J., Simultaneous determination of 16 synthetic colorants in hotpot condiment by high performance liquid chromatography. *Journal of Chromatography B* **2014,** *960*, 87-91.
30. Takhar, M.; Stroud, C. A.; Chan, A. W., Volatility Distribution and Evaporation Rates of Organic Aerosol from Cooking Oils and their Evolution upon Heterogeneous Oxidation. *ACS Earth and Space Chemistry* **2019,** *3*, (9), 1717-1728.
31. Li, J.; Liu, Q.; Li, Y.; Liu, T.; Huang, D.; Zheng, J.; Zhu, W.; Hu, M.; Wu, Y.; Lou, S., Characterization of aerosol aging potentials at suburban sites in northern and southern China utilizing a potential aerosol mass (Go: PAM) reactor and an aerosol mass spectrometer. *Journal of Geophysical Research: Atmospheres* **2019,** *124*, (10), 5629-5649.
32. Watne, Å. K.; Psichoudaki, M.; Ljungström, E.; Le Breton, M.; Hallquist, M.; Jerksjö, M.; Fallgren, H.; Jutterström, S.; Hallquist, Å. M., Fresh and oxidized emissions from in-use transit buses running on diesel, biodiesel, and CNG. *Environmental science & technology* **2018,** *52*, (14), 7720-7728.
33. Choe, E.; Min, D., Chemistry of deep-fat frying oils. *Journal of food science* **2007,** *72*, (5), R77-R86.
34. Zhang, Q.; Saleh, A. S.; Chen, J.; Shen, Q., Chemical alterations taken place during deep-fat frying based on certain reaction products: A review. *Chemistry and physics of lipids* **2012,** *165*, (6), 662-681.
35. Lindinger, W.; Hansel, A.; Jordan, A., On-line monitoring of volatile organic compounds at pptv levels by means of proton-transfer-reaction mass spectrometry (PTR-MS) medical applications, food control and environmental research. *International Journal of Mass Spectrometry and Ion Processes* **1998,** *173*, (3), 191-241.
36. Cui, L.; Zhang, Z.; Huang, Y.; Lee, S. C.; Blake, D. R.; Ho, K. F.; Wang, B.; Gao, Y.; Wang, X. M.; Louie, P. K. K., Measuring OVOCs and VOCs by PTR-MS in an urban roadside microenvironment of Hong Kong: relative humidity and temperature dependence, and field intercomparisons. *Atmospheric Measurement Techniques* **2016,** *9*, (12), 5763-5779.

37. Holm, E.; Adamsen, A.; Feilberg, A.; Schäfer, A.; Løkke, M.; Petersen, M., Quality changes during storage of cooked and sliced meat products measured with PTR-MS and HS-GC–MS. *Meat science* **2013,** *95*, (2), 302-310.
38. Liu, T.; Wang, X.; Hu, Q.; Deng, W.; Zhang, Y.; Ding, X.; Fu, X.; Bernard, F.; Zhang, Z.; Lü, S., Formation of secondary aerosols from gasoline vehicle exhaust when mixing with SO 2. *Atmospheric Chemistry and Physics* **2016,** *16*, (2), 675-689.
39. Mao, J.; Ren, X.; Brune, W.; Olson, J.; Crawford, J.; Fried, A.; Huey, L.; Cohen, R.; Heikes, B.; Singh, H., Airborne measurement of OH reactivity during INTEX-B. *Atmospheric Chemistry and Physics* **2009,** *9*, (1), 163-173.
40. Zhang, Q.; Canagaratna, M. R.; Jayne, J. T.; Worsnop, D. R.; Jimenez, J. L., Time-and size-resolved chemical composition of submicron particles in Pittsburgh: Implications for aerosol sources and processes. *Journal of Geophysical Research: Atmospheres* **2005,** *110*, (D7).
41. DeCarlo, P. F.; Kimmel, J. R.; Trimborn, A.; Northway, M. J.; Jayne, J. T.; Aiken, A. C.; Gonin, M.; Fuhrer, K.; Horvath, T.; Docherty, K. S., Field-deployable, high-resolution, time-of-flight aerosol mass spectrometer. *Analytical chemistry* **2006,** *78*, (24), 8281-8289.
42. Reyes-Villegas, E.; Bannan, T.; Le Breton, M.; Mehra, A.; Priestley, M.; Percival, C.; Coe, H.; Allan, J. D., Online chemical characterization of food-cooking organic aerosols: implications for source apportionment. *Environmental science & technology* **2018,** *52*, (9), 5308-5318.
43. Canagaratna, M.; Jimenez, J.; Kroll, J.; Chen, Q.; Kessler, S.; Massoli, P.; Hildebrandt Ruiz, L.; Fortner, E.; Williams, L.; Wilson, K., Elemental ratio measurements of organic compounds using aerosol mass spectrometry: characterization, improved calibration, and implications. *Atmospheric Chemistry and Physics* **2015,** *15*, (1), 253-272.
44. Aiken, A. C.; Decarlo, P. F.; Kroll, J. H.; Worsnop, D. R.; Huffman, J. A.; Docherty, K. S.; Ulbrich, I. M.; Mohr, C.; Kimmel, J. R.; Sueper, D., O/C and OM/OC ratios of primary, secondary, and ambient organic aerosols with high-resolution time-of-flight aerosol mass spectrometry. *Environmental science & technology* **2008,** *42*, (12), 4478-4485.
45. Aiken, A. C.; DeCarlo, P. F.; Jimenez, J. L., Elemental analysis of organic species with electron ionization high-resolution mass spectrometry. *Analytical chemistry* **2007,** *79*, (21), 8350-8358.
46. Liu, T.; Liu, Q.; Li, Z.; Huo, L.; Chan, M.; Li, X.; Zhou, Z.; Chan, C. K., Emission of volatile organic compounds and production of secondary organic aerosol from stir-frying spices. *Science of the Total Environment* **2017,** *599*, 1614-1621.
47. Gao, J.; Cao, C.; Wang, L.; Song, T.; Zhou, X.; Yang, J.; Zhang, X., Determination of size-dependent source emission rate of cooking-generated aerosol particles at the oil-heating stage in an experimental kitchen. *Aerosol and Air Quality Research* **2012,** *13*, (2), 488-496.
48. Torkmahalleh, M. A.; Goldasteh, I.; Zhao, Y.; Udochu, N. M.; Rossner, A.; Hopke, P.; Ferro, A., PM2. 5 and ultrafine particles emitted during heating of commercial cooking oils. *Indoor Air* **2012,** *22*, (6), 483-491.
49. America, C. I. o., *The professional chef*. Institutions/Volume feeding magazine: 1974.
50. Zhu, X.; Wang, K.; Zhu, J.; Koga, M., Analysis of cooking oil fumes by ultraviolet spectrometry and gas chromatography− mass spectrometry. *Journal of Agricultural and Food Chemistry* **2001,** *49*, (10), 4790-4794.
51. Gunstone, F., The major sources of oils, fats, and other lipids. In *Fatty Acid and Lipid Chemistry*, Springer: 1996; pp 61-86.
52. Chyau, C.-C.; Mau, J.-L., Effects of various oils on volatile compounds of deep-fried shallot flavouring. *Food chemistry* **2001,** *74*, (1), 41-46.

53. Liu, X., The effect of temperature and heating time on the formation of alpha, beta unsaturated hydroxyaldehydes in various vegetable oils and fats. **2014**.
54. Yasuhara, A.; Shibamoto, T., Analysis of aldehydes and ketones in the headspace of heated pork fat. *Journal of food science* **1989,** *54*, (6), 1471-1472.
55. Liu, H.; Wang, Z.; Zhang, D.; Shen, Q.; Hui, T.; Ma, J., Generation of key aroma compounds in Beijing roasted duck induced via Maillard reaction and lipid pyrolysis reaction. *Food Research International* **2020,** *136*, 109328.
56. Katragadda, H. R.; Fullana, A.; Sidhu, S.; Carbonell-Barrachina, Á. A., Emissions of volatile aldehydes from heated cooking oils. *Food Chemistry* **2010,** *120*, (1), 59-65.
57. Katsuta, I.; Shimizu, M.; Yamaguchi, T.; Nakajima, Y., Emission of volatile aldehydes from DAG-rich and TAG-rich oils with different degrees of unsaturation during deep-frying. *Journal of the American Oil Chemists' Society* **2008,** *85*, (6), 513-519.
58. Fullana, A.; Carbonell-Barrachina, Á. A.; Sidhu, S., Volatile aldehyde emissions from heated cooking oils. *Journal of the Science of Food and Agriculture* **2004,** *84*, (15), 2015-2021.
59. Chen, H.; Cao, P.; Li, B.; Sun, D.; Wang, Y.; Li, J.; Liu, Y., Effect of water content on thermal oxidation of oleic acid investigated by combination of EPR spectroscopy and SPME-GC-MS/MS. *Food chemistry* **2017,** *221*, 1434-1441.
60. Umano, K.; Shibamoto, T., Analysis of acrolein from heated cooking oils and beef fat. *Journal of Agricultural and Food Chemistry* **1987,** *35*, (6), 909-912.
61. Kostenidou, E.; Lee, B.-H.; Engelhart, G. J.; Pierce, J. R.; Pandis, S. N., Mass spectra deconvolution of low, medium, and high volatility biogenic secondary organic aerosol. *Environmental science & technology* **2009,** *43*, (13), 4884-4889.
62. Mohr, C.; Huffman, J. A.; Cubison, M. J.; Aiken, A. C.; Docherty, K. S.; Kimmel, J. R.; Ulbrich, I. M.; Hannigan, M.; Jimenez, J. L., Characterization of primary organic aerosol emissions from meat cooking, trash burning, and motor vehicles with high-resolution aerosol mass spectrometry and comparison with ambient and chamber observations. *Environmental Science & Technology* **2009,** *43*, (7), 2443-2449.
63. Shah, R. U.; Robinson, E. S.; Gu, P.; Robinson, A. L.; Apte, J. S.; Presto, A. A., High-spatial-resolution mapping and source apportionment of aerosol composition in Oakland, California, using mobile aerosol mass spectrometry. *Atmospheric Chemistry and Physics* **2018,** *18*, (22), 16325-16344.
64. Äijälä, M.; Heikkinen, L.; Fröhlich, R.; Canonaco, F.; Prévôt, A. S.; Junninen, H.; Petäjä, T.; Kulmala, M.; Worsnop, D.; Ehn, M., Resolving anthropogenic aerosol pollution types–deconvolution and exploratory classification of pollution events. *Atmospheric Chemistry and Physics* **2017,** *17*, (4), 3165-3197.
65. Struckmeier, C.; Drewnick, F.; Fachinger, F.; Gobbi, G. P.; Borrmann, S., Atmospheric aerosols in Rome, Italy: sources, dynamics and spatial variations during two seasons. *Atmospheric Chemistry and Physics* **2016,** *16*, (23), 15277-15299.
66. Hu, W.; Hu, M.; Hu, W.; Jimenez, J. L.; Yuan, B.; Chen, W.; Wang, M.; Wu, Y.; Chen, C.; Wang, Z., Chemical composition, sources, and aging process of submicron aerosols in Beijing: Contrast between summer and winter. *Journal of Geophysical Research: Atmospheres* **2016,** *121*, (4), 1955-1977.
67. Elser, M.; Huang, R.-J.; Wolf, R.; Slowik, J. G.; Wang, Q.; Canonaco, F.; Li, G.; Bozzetti, C.; Daellenbach, K. R.; Huang, Y., New insights into PM 2.5 chemical composition and sources in two major cities in China during extreme haze events using aerosol mass spectrometry. *Atmospheric Chemistry and Physics* **2016,** *16*, (5), 3207-3225.

68. Hayes, P.; Ortega, A.; Cubison, M.; Froyd, K.; Zhao, Y.; Cliff, S.; Hu, W.; Toohey, D.; Flynn, J.; Lefer, B., Organic aerosol composition and sources in Pasadena, California, during the 2010 CalNex campaign. *Journal of Geophysical Research: Atmospheres* **2013,** *118*, (16), 9233-9257.
69. Crippa, M.; El Haddad, I.; Slowik, J. G.; DeCarlo, P. F.; Mohr, C.; Heringa, M. F.; Chirico, R.; Marchand, N.; Sciare, J.; Baltensperger, U., Identification of marine and continental aerosol sources in Paris using high resolution aerosol mass spectrometry. *Journal of Geophysical Research: Atmospheres* **2013,** *118*, (4), 1950-1963.
70. Hu, W. W.; Hu, M.; Yuan, B.; Jimenez, J. L.; Tang, Q.; Peng, J.; Hu, W.; Shao, M.; Wang, M.; Zeng, L., Insights on organic aerosol aging and the influence of coal combustion at a regional receptor site of central eastern China. *Atmospheric Chemistry and Physics* **2013,** *13*, (19), 10095-10112.
71. Ng, N.; Canagaratna, M.; Jimenez, J.; Zhang, Q.; Ulbrich, I.; Worsnop, D., Real-time methods for estimating organic component mass concentrations from aerosol mass spectrometer data. *Environmental science & technology* **2011,** *45*, (3), 910-916.
72. Atkinson, R.; Arey, J., Atmospheric degradation of volatile organic compounds. *Chemical reviews* **2003,** *103*, (12), 4605-4638.
73. Nah, T.; Kessler, S. H.; Daumit, K. E.; Kroll, J. H.; Leone, S. R.; Wilson, K. R., OH-initiated oxidation of sub-micron unsaturated fatty acid particles. *Physical Chemistry Chemical Physics* **2013,** *15*, (42), 18649-18663.
74. Molina, M.; Ivanov, A.; Trakhtenberg, S.; Molina, L., Atmospheric evolution of organic aerosol. *Geophysical Research Letters* **2004,** *31*, (22).
75. Lambe, A.; Chhabra, P.; Onasch, T.; Brune, W.; Hunter, J.; Kroll, J.; Cummings, M.; Brogan, J.; Parmar, Y.; Worsnop, D., Effect of oxidant concentration, exposure time, and seed particles on secondary organic aerosol chemical composition and yield. *Atmospheric Chemistry and Physics* **2015,** *15*, (6), 3063-3075.
76. Chan, A.; Chan, M.; Surratt, J.; Chhabra, P.; Loza, C.; Crounse, J.; Yee, L.; Flagan, R.; Wennberg, P.; Seinfeld, J., Role of aldehyde chemistry and NO x concentrations in secondary organic aerosol formation. *Atmospheric Chemistry and Physics* **2010,** *10*, (15), 7169-7188.
77. Gao, T.; Andino, J. M.; Rivera, C. C.; Márquez, M. F., Rate constants of the gas-phase reactions of OH radicals with trans-2-hexenal, trans-2-octenal, and trans-2-nonenal. *International Journal of Chemical Kinetics* **2009,** *41*, (7), 483-489.
78. Davis, M.; Gilles, M.; Ravishankara, A.; Burkholder, J. B., Rate coefficients for the reaction of OH with (E)-2-pentenal,(E)-2-hexenal, and (E)-2-heptenal. *Physical Chemistry Chemical Physics* **2007,** *9*, (18), 2240-2248.
79. Magneron, I.; Thevenet, R.; Mellouki, A.; Le Bras, G.; Moortgat, G.; Wirtz, K., A study of the photolysis and OH-initiated oxidation of acrolein and trans-crotonaldehyde. *The Journal of Physical Chemistry A* **2002,** *106*, (11), 2526-2537.
80. Chacon-Madrid, H. J.; Presto, A. A.; Donahue, N. M., Functionalization vs. fragmentation: n-aldehyde oxidation mechanisms and secondary organic aerosol formation. *Physical Chemistry Chemical Physics* **2010,** *12*, (42), 13975-13982.
81. Singh, A.; Satish, R. V.; Rastogi, N., Characteristics and sources of fine organic aerosol over a big semi-arid urban city of western India using HR-ToF-AMS. *Atmospheric Environment* **2019,** *208*, 103-112.
82. Li, Y.; Lee, B. P.; Su, L.; Fung, J. C. H.; Chan, C. K., Seasonal characteristics of fine particulate matter (PM) based on high-resolution time-of-flight aerosol mass spectrometric (HR-

ToF-AMS) measurements at the HKUST Supersite in Hong Kong. *Atmospheric Chemistry and Physics* **2015,** *15*, (1), 37-53.
83. Liu, T.; Zhou, L.; Liu, Q.; Lee, B. P.; Yao, D.; Lu, H.; Lyu, X.; Guo, H.; Chan, C. K., Secondary organic aerosol formation from urban roadside air in Hong Kong. *Environmental science & technology* **2019,** *53*, (6), 3001-3009.
84. Zhou, L.; Hallquist, Å. M.; Hallquist, M.; Salvador, C. M.; Gaita, S. M.; Sjödin, Å.; Jerksjö, M.; Salberg, H.; Wängberg, I.; Mellqvist, J., A transition of atmospheric emissions of particles and gases from on-road heavy-duty trucks. *Atmospheric Chemistry and Physics* **2020,** *20*, (3), 1701-1722.
85. Bishop, G. A.; Hottor-Raguindin, R.; Stedman, D. H.; McClintock, P.; Theobald, E.; Johnson, J. D.; Lee, D.-W.; Zietsman, J.; Misra, C., On-road heavy-duty vehicle emissions monitoring system. *Environmental science & technology* **2015,** *49*, (3), 1639-1645.
86. Zhao, Y.; Lambe, A. T.; Saleh, R.; Saliba, G.; Robinson, A. L., Secondary organic aerosol production from gasoline vehicle exhaust: effects of engine technology, cold start, and emission certification standard. *Environmental science & technology* **2018,** *52*, (3), 1253-1261.
87. Abdullahi, K. L.; Delgado-Saborit, J. M.; Harrison, R. M., Emissions and indoor concentrations of particulate matter and its specific chemical components from cooking: A review. *Atmospheric Environment* **2013,** *71*, 260-294.

676 **Graphic for Table of Contents (TOC)**

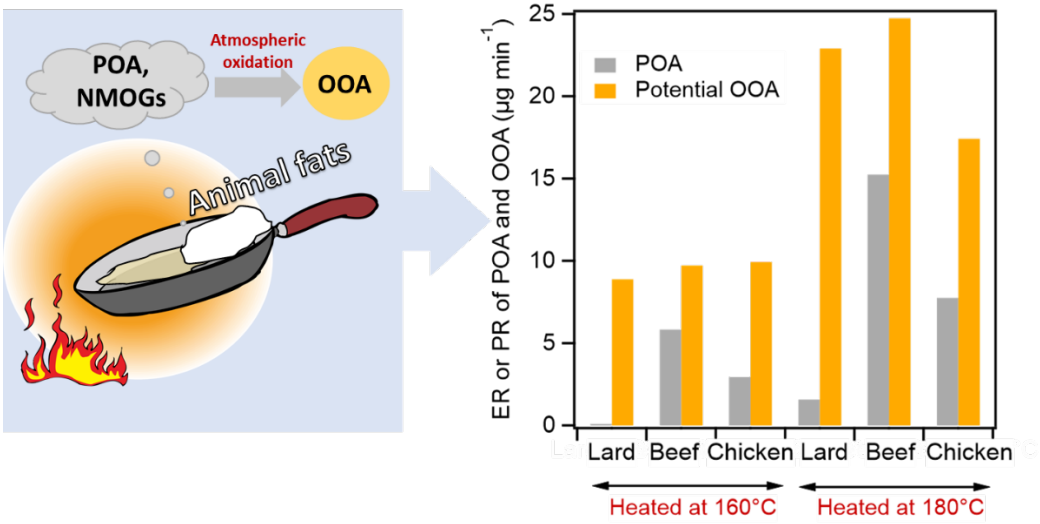

677

678

679

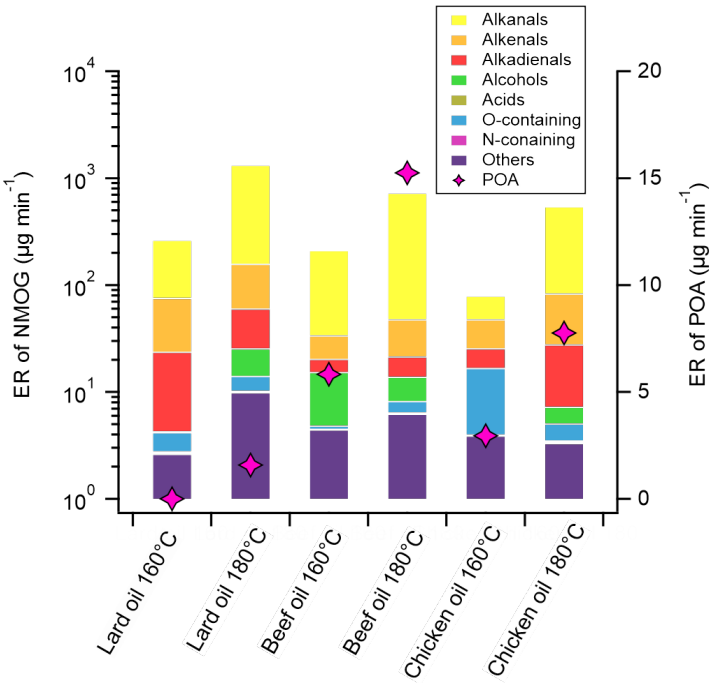

680 **Figure 1.** Emission rates of NMOGs and POA from different heated animal fats at 160 and 180°C.

681

682

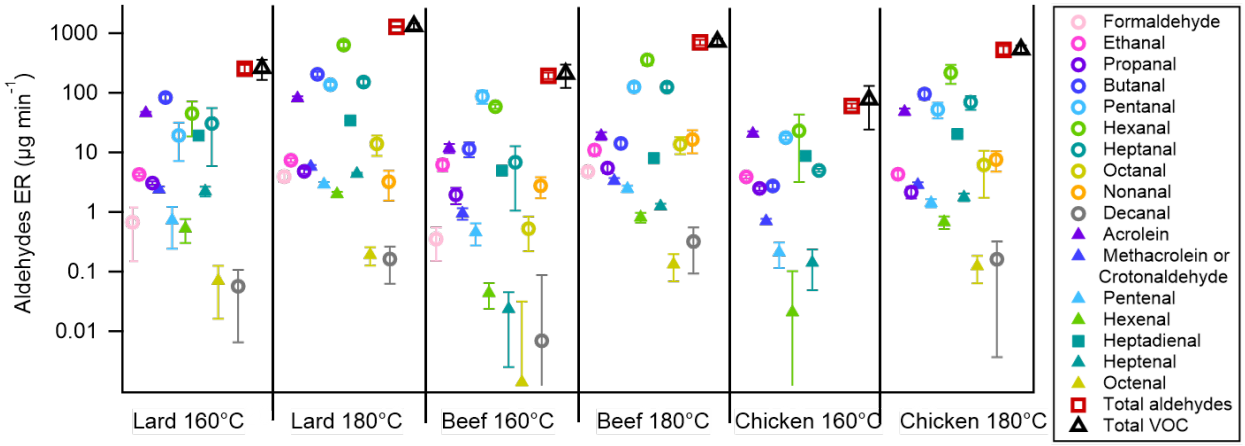

683

684 **Figure 2.** Speciation and distribution of aldehydes from the heated animal fats at 160 and 180°C.

685 Error bars represent the standard deviation (1σ).

686

687

688 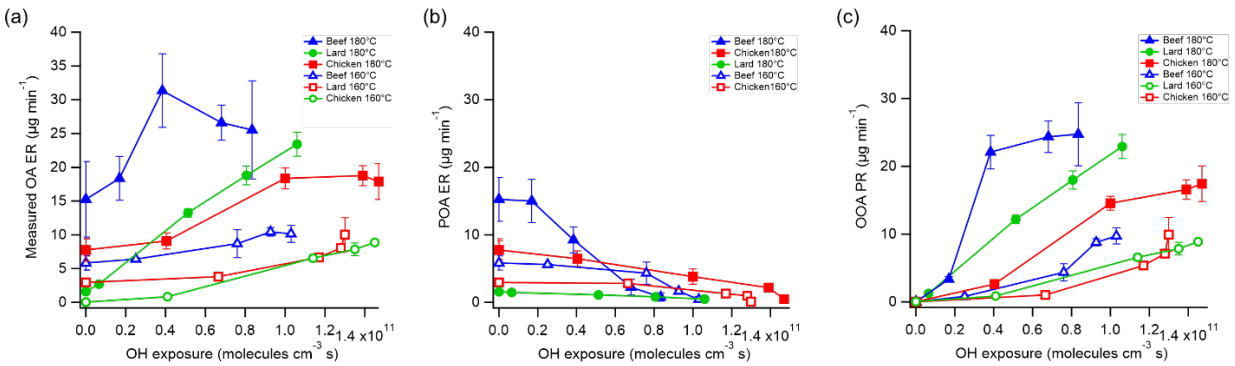

689 **Figure 3.** (a) Measured OA ER, and (b) POA factor ER and (c) OOA factor PR from the PMF
690 analysis of the emission oxidation experiments of heated animal fats at 160 and 180°C as a function
691 of OHexp. For 160 °C lard, two PMF OOA factors were combined in Figure 3c. Error bars
692 represent the standard deviation (1σ).

693

694

695

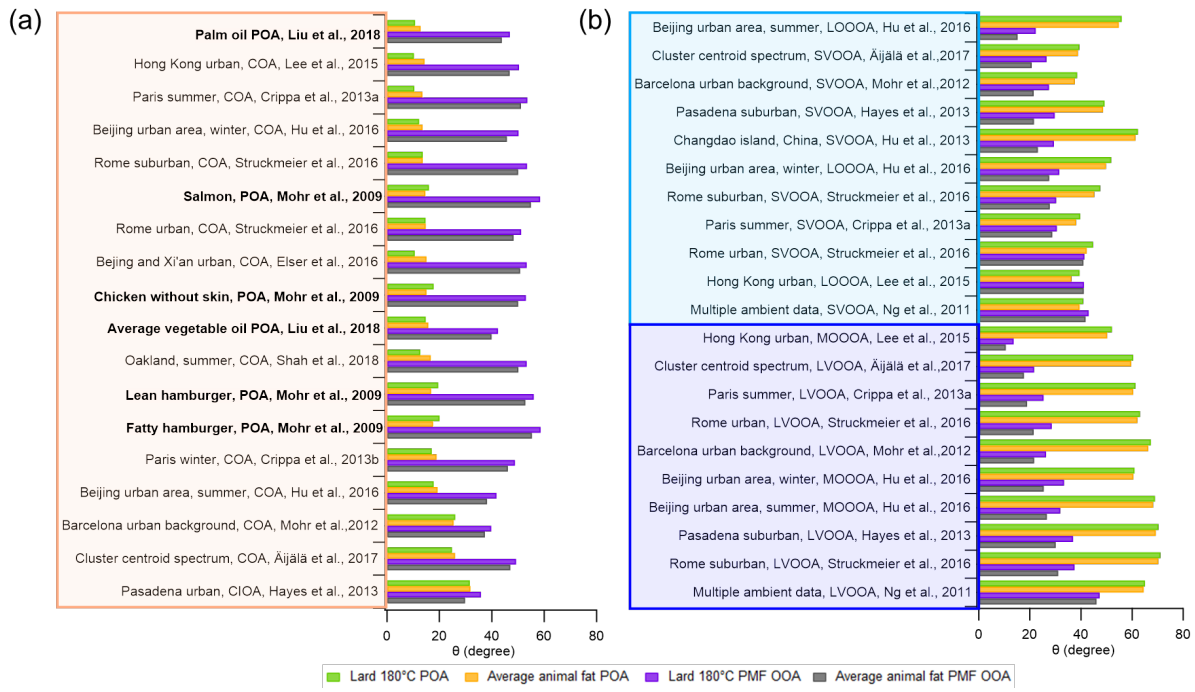

Figure 4. Angles (θ) between (a) ambient COA factor[5-7, 63-69] and laboratory-generated cooking POA[23, 62] mass spectra, (b) ambient SVOOA, LOOOA, MOOOA and LVOOA factor[5, 7, 64-66, 68-71] mass spectra and the 180°C lard POA mass spectrum, average animal fat POA mass spectrum, 180°C lard PMF OOA factor spectrum, and average animal fat PMF OOA factor spectrum. The average POA mass spectrum was averaged for lard (180°C), beef (160 and 180°C) and chicken fats (160 and 180°C). The average PMF OOA spectrum was averaged for lard (160 and 180°C), beef (160 and 180°C) and chicken fats (160 and 180°C). Laboratory studies were marked in bold. COA, SVOOA, LOOOA, MOOOA and LVOOA indicated cooking organic aerosol, semi-volatile oxygenated organic aerosol, less oxidized oxygenated organic aerosol, more oxidized oxygenated organic aerosol and low volatility oxygenated organic aerosol, respectively.

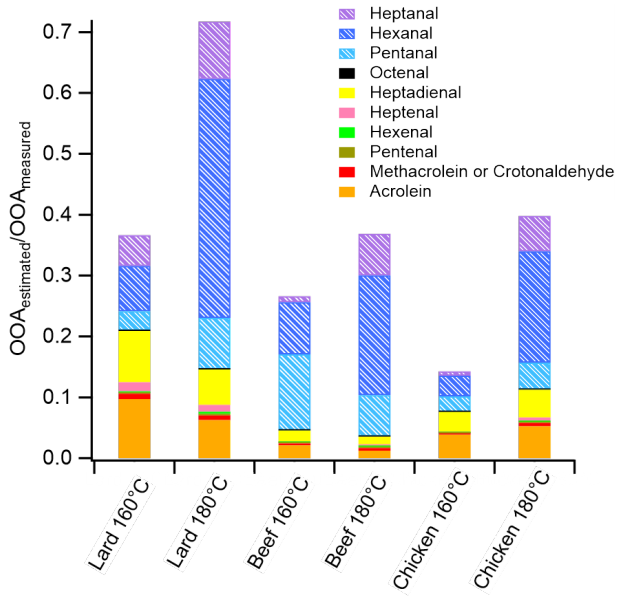

709

710 **Figure 5.** Estimated contributions of individual alkenals and alkanals to observed OOA for heated
711 animal fats at 160 and 180°C. The abundance of heptadienal was estimated based on its good
712 correlation with acrolein (R^2=0.97) in Liu et al. [15].

713

714

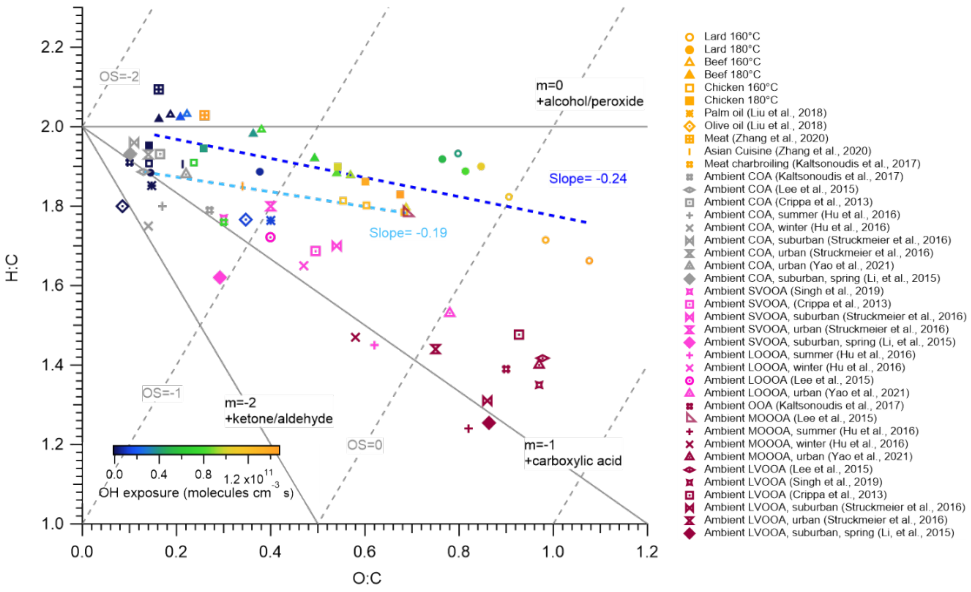

Figure 6. Van Krevelen diagram of OA from different animal fats, vegetable oils[23], meat frying[24] or charbroiling[21] and Asian cuisine[24] as well as ambient PMF COA and OOA factors[4, 5, 21, 65, 66, 69, 81, 82]. COA, SVOOA, LOOOA, MOOOA and LVOOA indicated cooking organic aerosol, semi-volatile oxygenated organic aerosol, less oxidized oxygenated organic aerosol, more oxidized oxygenated organic aerosol and low volatility oxygenated organic aerosol, respectively.